Proceedings of the ASME 2010 3rd Joint US-European Fluids Engineering Summer Meeting and 8th International Conference on Nanochannels, Microchannels, and Minichannels
FEDSM-ICNMM2010
August 1-5, 2010, Montreal, Canada

FEDSM-ICNMM2010-30888

NUMERICAL SIMULATION OF THE FLOW AROUND A CIRCULAR CYLINDER FOLLOWING A FIGURE-8-LIKE PATH

László Baranyi
Department of Fluid and Heat Engineering,
University of Miskolc
3515 Miskolc-Egyetemváros, Hungary
E-mail: arambl@uni-miskolc.hu

ABSTRACT

This numerical study investigates a circular cylinder placed in a uniform stream and moving along a slender figure-8 path. A 2D computational method based on the finite difference method was used. Two aspects were investigated separately: the effect of in-line amplitude of oscillation and the effect of the frequency ratio. Computations for varying amplitude values were carried out at Re=150, 200 and 250. Time-mean and rms values of force coefficients yielded smooth curves and tended to increase with amplitude.

When plotted against frequency ratio in the domain of 0.69 to 0.98 at Re=250, a jump was found in the time-mean values of lift and torque. This was also present in the energy transfer curves, and positive and negative values were found.

Limit cycle curves from before and after a jump were symmetric, mirror images, and quite complex. Vorticity contours also showed a mirror image pre- and post-jump. These results indicate the possibility of symmetry-breaking bifurcation.

Keywords: circular cylinder, figure-8, forced oscillation, lock-in

INTRODUCTION

Flow around a circular cylinder is very rich in flow phenomena, and this is even more so the case when the cylinder is oscillating. Many studies have been devoted to oscillating cylinders, among them Williamson and Roshko (1988), Lu and Dalton (1996), and Blackburn and Henderson (1999) for transverse oscillation. In-line oscillation has been investigated in Cetiner and Rockwell (2001), Al-Mdallal et al. 2007, Mureithi et al. (2009), and many others.

In practice, it can happen that oscillation occurs not only in transverse direction, but simultaneously occurs in in-line direction as well. When the frequencies for the two oscillations are equal to each other, an elliptical path is obtained. Such orbital motion has been investigated in Didier and Borges (2007), Baranyi (2008), and Stansby and Rainey (2001), for instance. Baranyi identified sudden switches in vortex structure while varying the amplitude of oscillation.

It can also occur that the cylinder oscillates in in-line direction at twice the frequency of the transverse oscillation, leading to a figure-8-like path. Perdikaris et al. (2009) investigated such a case at Re=400 while varying the transverse amplitude of oscillation. Their study looked at the power transfer parameter for two frequency ratios of 0.5 and 1. They found that the orientation of the motion (clockwise or counter-clockwise) influences the results.

This study investigates flow around a circular cylinder following a figure-8-shaped path in order to gain a better understanding of the effect of parameters such as amplitude and frequency ratio on flow phenomena.

NOMENCLATURE

$A_{x,y}$	amplitude of oscillation in x or y directions, respectively, non-dimensionalized by d
C_D	drag coefficient, $2F_D/(\rho U^2 d)$
C_L	lift coefficient, $2F_L/(\rho U^2 d)$
C_{pb}	base pressure coefficient
d	cylinder diameter (m)
E	mechanical energy transfer, non-dimensionalized by $\rho U^2 d^2/2$
$\mathbf{F}$	force per unit length of cylinder, $F_D\,\mathbf{i} + F_L\,\mathbf{j}$ (N/m)
F_D	drag per unit length of cylinder (N/m)
F_L	lift per unit length of cylinder (N/m)
f	oscillation frequency, non-dimensionalized by U/d
i, j	unit vectors in x and y directions, respectively

p non-dimensionalized by ρU^2
Re Reynolds number, Ud/ν
R radius, non-dimensionalized by d
St non-dimensional vortex shedding frequency
T motion period, non-dimensionalized by d/U
t time, non-dimensionalized by d/U
tq torque coefficient, torque of shear stress on cylinder surface, non-dimensionalized by $\rho U^2 d^2$
U free stream velocity, velocity scale (m/s)
$\mathbf{v}_0$ cylinder velocity, non-dimensionalized by U
x,y Cartesian co-ordinates, non-dimensionalized by d
ν kinematic viscosity (m^2/s)
Θ polar angle characterizing initial condition
ρ fluid density (kg/m^3)

Subscripts

fb fixed body
D drag
L lift
mean time-mean value
rms root-mean-square value
x, *y* components in *x* and *y* directions
1, 2 for energy transfer in *y* and *x* directions, respectively
0 for cylinder motion; for stationary cylinder at same Re

COMPUTATIONAL METHOD

A non-inertial system fixed to the cylinder is used to compute 2D low-Reynolds number unsteady flow around a circular cylinder placed in a uniform stream and forced to oscillate in transverse, in in-line direction, or both. The non-dimensional Navier-Stokes equations for incompressible constant-property Newtonian fluid, the equation of continuity and the Poisson equation for pressure can be written as follows, equations (1) to (4):

$$\frac{\partial u}{\partial t}+u\frac{\partial u}{\partial x}+v\frac{\partial u}{\partial y}=-\frac{\partial p}{\partial x}+\frac{1}{\mathrm{Re}}\nabla^2 u-a_{0x} \quad (1)$$

$$\frac{\partial v}{\partial t}+u\frac{\partial v}{\partial x}+v\frac{\partial v}{\partial y}=-\frac{\partial p}{\partial y}+\frac{1}{\mathrm{Re}}\nabla^2 v-a_{0y} \quad (2)$$

$$D=\frac{\partial u}{\partial x}+\frac{\partial v}{\partial y}=0 \quad (3)$$

$$\frac{\partial^2 p}{\partial x^2}+\frac{\partial^2 p}{\partial y^2}=2\left[\frac{\partial u}{\partial x}\frac{\partial v}{\partial y}-\frac{\partial u}{\partial y}\frac{\partial v}{\partial x}\right]-\frac{\partial D}{\partial t} \quad (4)$$

In these equations, u and v are the x and y components of velocity, t is time, p is the pressure, Re is the Reynolds number based on cylinder diameter d, free stream velocity U, and kinematic viscosity ν, and D is the dilation. Although D is theoretically equal to 0 from equation (3), it is kept in equation (4) to avoid accumulation of numerical errors. In equations (1) and (2) a_{0x} and a_{0y} mean the x and y components of cylinder acceleration, respectively.

On the cylinder surface, no-slip boundary condition is used for the velocity and a Neumann type boundary condition is used for the pressure. At the far region, potential flow is assumed.

Boundary-fitted coordinates are used to impose the boundary conditions accurately. Using unique, single-valued functions, the physical domain bounded by two concentric circles is mapped into a rectangular computational domain with equidistant spacing in both directions (see Fig. 1). In the physical domain logarithmically spaced radial cells are used, providing a fine grid scale near the cylinder wall and a coarse grid in the far field. The transformed governing equations and boundary conditions are solved by finite difference method. Space derivatives are approximated by fourth order central differences, except for the convective terms for which a third order modified upwind scheme is used. The Poisson equation for pressure is solved by the successive over-relaxation (SOR) method. The Navier-Stokes equations are integrated explicitly and continuity is satisfied at every time step. For further details see Baranyi (2003; 2008).

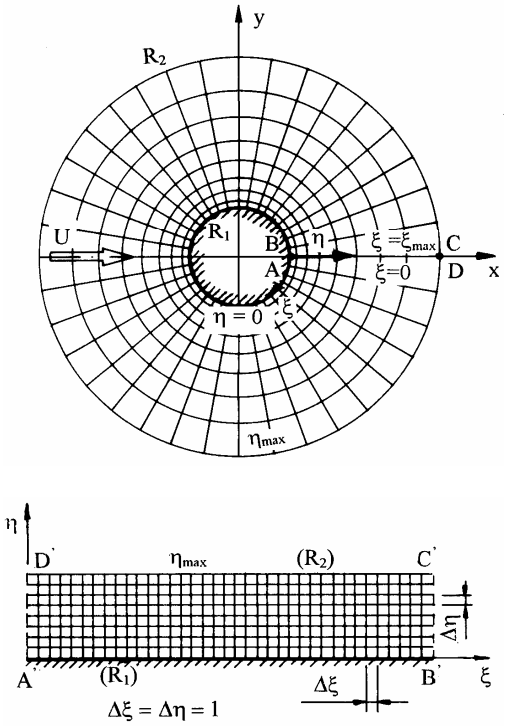

Figure 1. Physical and computational domains

The 2D code developed by the author has been extensively tested against experimental and computational results for a stationary cylinder (e.g. Chakraborty et al., 2004, Baranyi, 2008) and computational results for cylinders oscillating in transverse or in in-line directions or following a circular path, including Lu and Dalton (1996), Al-Mdallal et al. (2007), and Didier and Borges (2007), with good agreement being found, (Baranyi, 2008). In this study the dimensionless time step is 0.0005, the number of grid points is 481x451, and a relatively large physical domain of R_2/R_1=360 has been chosen to enhance accuracy.

COMPUTATIONAL SETUP

This study investigates the behavior of flow past a cylinder placed in a uniform stream with its axis perpendicular to the velocity vector of the main flow. The cylinder is oscillated mechanically in both in-line and transverse directions in relation to the uniform stream. The motion of the centre of the cylinder is described by the following equations:

$$x_0=A_x \cos(2\pi f_x t+\Theta) \tag{5}$$

$$y_0= - A_y \sin(2\pi f_y t+\Theta) \tag{6}$$

where Θ is a polar angle characterizing the initial position of the cylinder. Naturally the second time derivatives of x_0 and y_0 give the accelerations a_{0x} and a_{0y} in equations (1) and (2).

The time-history of force coefficients (lift, drag, base pressure and torque), pressure and velocity field are computed. From these data, time-mean (TM) and root-mean-square (rms) values of force coefficients, streamlines, and vorticity contours can be obtained.

Throughout this paper the lift and drag coefficients used unless otherwise stated contain the inertial forces originated from the non-inertial system fixed to the accelerating cylinder. Coefficients obtained by removing the inertial forces are often termed 'fixed body' coefficients (see Lu and Dalton, 1996). The relationship between the two sets of coefficients can be written as

$$C_D=C_{D\,fb} +\pi\, a_{0x} / 2 \tag{7}$$

$$C_L=C_{L\,fb} +\pi\, a_{0y} / 2 \tag{8}$$

where subscript 'fb' refers to the fixed body (understood in an inertial system fixed to the stationary cylinder), Baranyi (2005). Since the inertial terms are T-periodic functions, their time-mean values vanish, resulting in identical TM values for lift and drag in the inertial and non-inertial systems. Naturally the rms values of C_L and C_D will be somewhat different in the two systems (but this does not affect the curve being continuous).

Investigation was restricted to lock-in cases. Lock-in, or the synchronization between vortex shedding and cylinder motion, produces a periodic solution for each of the force coefficients. In this paper, we consider lock-in to be when the vortex shedding frequency is identical to f_y, the frequency of transverse cylinder oscillation.

To create a figure-8 path with a clockwise orientation in the upper loop, conditions

$$f_x=2 f_y; \quad \Theta =- \pi / 2$$

should be fulfilled in equations (5) and (6).

The non-dimensional energy transfer originally introduced by Blackburn and Henderson (1999) for transversely oscillated cylinder was extended for a general two-degree-of-freedom motion of the cylinder by Baranyi (2008):

$$E = \frac{2}{\rho U^2 d^2} \int_0^T \mathbf{F} \cdot \mathbf{v}_0 \,\mathrm{d}\, t = \int_0^T \left(C_D\, v_{0x} + C_L\, v_{0y}\right) \mathrm{d}\, t$$

where T is the motion period, v_{0x} and v_{0y} are the velocity of the cylinder in x and y directions, respectively. For transverse cylinder oscillation x_0=0, hence only the integral of the product of lift and transverse cylinder velocity component contributes to the energy transfer. This will be denoted by E_1, and that originating from the drag and in-line cylinder velocity component by E_2. The sum of E_1 and E_2 gives the mechanical energy transfer $E= E_1 + E$. Some researchers prefer to use non-dimensional power transfer (see Perdikaris et al., 2009) instead of the energy transfer coefficient E.

RESULTS

For a single computation, all parameters (A_x, A_y, Re, f_x, f_y, Θ) are kept constant. The computations are then repeated at different A_x values to investigate the effect of oscillation amplitude. A_y was set at 0.5, and A_x values between 0.1 and 0.2 were chosen in order to maintain an elongated path in the y direction, as this is said to be more relevant to actual engineering situations.

The same approach is used to investigate the effect of frequency ratio f_y / St_0. Here St_0 is the non-dimensional vortex shedding frequency from a stationary cylinder at the given Reynolds number. Only the locked-in domain was considered, which for Re=250 and A_x=0.14, A_y=0.5 was determined to be f_y / St_0=0.69 to 0.98.

For both cases, time-mean (TM) and root-mean-square (rms) values of lift (C_L), drag (C_D), base pressure (C_{pb}) and torque (tq) coefficients, further the mechanical energy transfer E between the cylinder and fluid were determined and plotted against the independent variable. The polar angle Θ was zero throughout the whole investigation.

Effect of In-line Amplitude

Here, three Re values were investigated: Re=150, 200, and 250. The frequency of transverse oscillation was kept at f_y/St_0 =0.9, under resonant forcing. This frequency ratio ensures moderate amplitude values for subharmonic lock-in. The dimensionless transverse amplitude of oscillation A_y was fixed at the value of 0.5 while A_x was varied systematically between 0.1 and 0.2.

Figure 2 shows the variation of TM of lift against A_x for the three Re values. As seen in the figure, all TM values of lift in the domain are positive and the values increase with both A_x and Reynolds number.

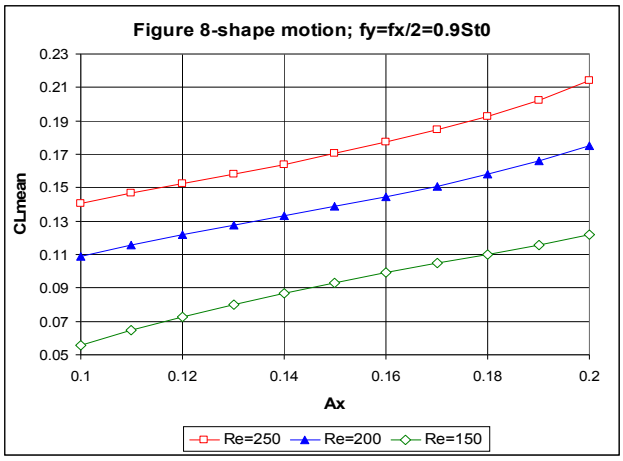

Figure 2. Time-mean value of lift vs. A_x for Re=150, 200 and 250

Figure 3 shows the variation of rms value of fixed body (see equations (7) and (8)) lift coefficient against A_x for the three Re values. The trend for these curves is very similar to that shown in Fig. 2. Other TM and rms curves show the same trend, with the exception of the TM of the torque coefficient, shown in Fig. 4, where no general tendency can be ascertained yet.

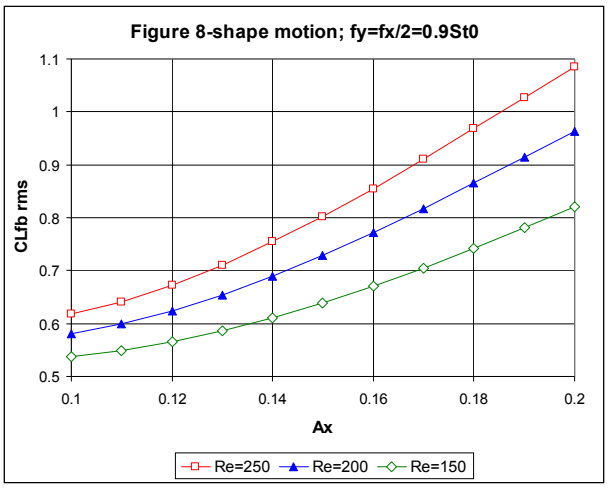

Figure 3. Rms value of fixed body lift vs. A_x for Re=150, 200 and 250

Note that no jumps indicating vortex switches were found within this parameter domain, in contrast to findings for an orbiting cylinder (see Baranyi, 2008) or cylinder moving in-line (Baranyi, 2009), meaning that no bifurcation was found within this domain.

Finally, Fig. 5 shows the variation of E with A_x for the three Reynolds numbers. This mechanical energy transfer was negative for all the investigated cases, meaning that energy is transferred from the cylinder to the fluid. The absolute value of E increases with increasing amplitude A_x. As can be seen in the figure, the relationship between E and A_x for the two smaller Reynolds numbers is almost linear. It can also be observed that the order of the absolute value of E values at the two ends of the A_x domain is reversed. Since all energy transfer values are negative, no vortex-induced vibration can occur.

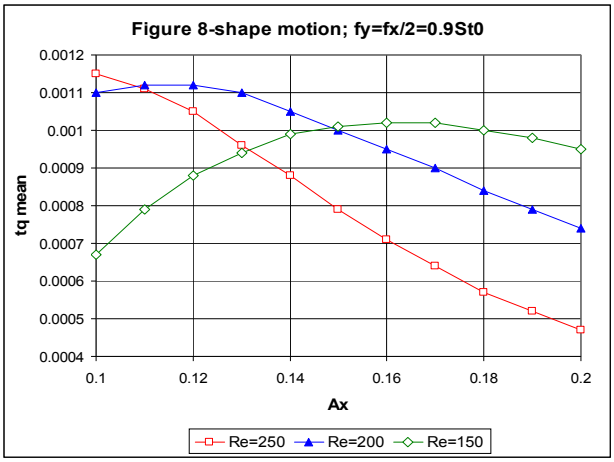

Figure 4. Time-mean value of torque vs. A_x for Re=150, 200 and 250

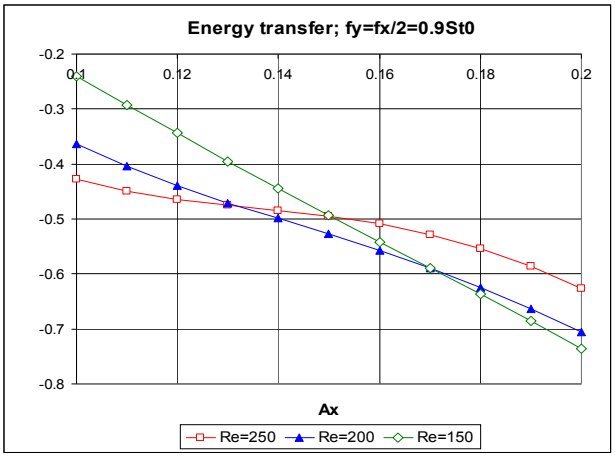

Figure 5. Mechanical energy transfer E vs. A_x for Re=150, 200 and 250

Effect of Frequency Ratio

Here, only one Reynolds number was investigated, Re=250. A_y was chosen to be 0.5, A_x was 0.14 during the whole investigation. The step between two consecutive frequency ratio f_y / St_0 values was 0.01, except around the area of the jump, where computations were carried out at smaller intervals to determine the location of the jump. The locked-in domain ranged from f_y / St_0=0.69 to 0.98.

Figure 6 shows the TM of lift. As can be seen, at around 0.71 there is a jump from negative values to positive values, and the absolute values are approximately equal to each other. Considering findings from earlier studies (Baranyi, 2008; 2009), there exist two so-called state curves that can be reproduced by varying the initial condition Θ. These state curves were found to be symmetric around zero (i.e., the value for a stationary cylinder) for in-line oscillation (Baranyi, 2009),

and this may be the case here, as well. If so, it is probably due to a symmetry-breaking bifurcation (see e.g., Crawford and Knobloch, 1991).

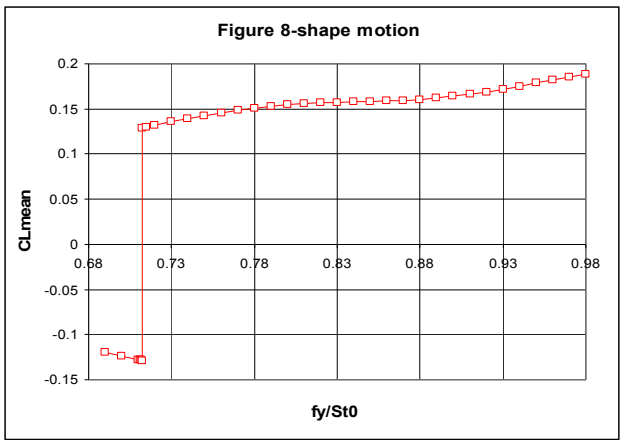

Figure 6. Time-mean value of lift vs. frequency ratio for Re=250

Three rms values of similar magnitudes are shown in Fig. 7. All values increase with increasing frequency ratio; the largest is the fixed body drag, followed by base pressure and the fixed body lift, while the rms of torque (not shown here) is about two orders of magnitude smaller, but also increases with frequency ratio.

Figure 8 gives the TM of torque, once again displaying the jump seen for the TM of lift shown in Fig. 6, with the jump being located at the same frequency ratio as for lift. The state curves are once again apparently symmetric. The fact that a jump was found in the TM of lift and torque only (out of the four TM and four rms curves of force coefficients) is characteristic also of the earlier results for in-line oscillation (Baranyi, 2009).

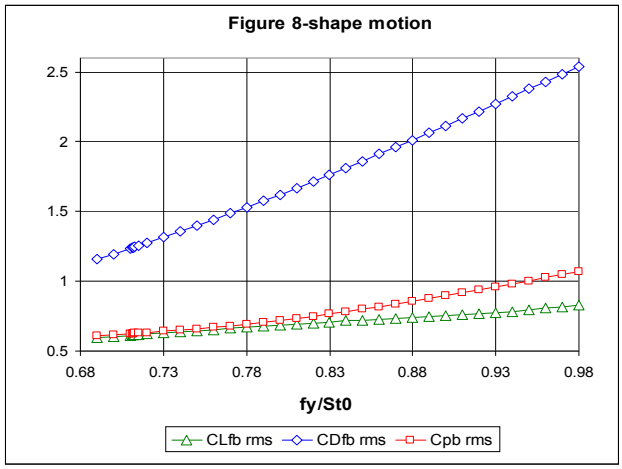

Figure 7. Rms values of base pressure, fixed-body lift and drag vs. frequency ratio for Re=250

The mechanical energy transfer, broken into its two components and their sum, is shown in Fig. 9. E_2 (originating from the product of drag and in-line cylinder velocity) is nearly constant—almost independent of the frequency ratio—and negative. E_1, related to transverse motion and force, also undergoes a jump, again at around f_y / St_0=0.71, and the two (incomplete) state curves appear to be symmetric. The sum of the two components, E, follows the shape of E_1 and can be either positive or negative. Below f_y / St_0=0.71, the cylinder obtains energy from the fluid, which might lead to vortex-induced vibration. Above this, however, E is always negative within the domain investigated, i.e., the fluid obtains energy from the cylinder.

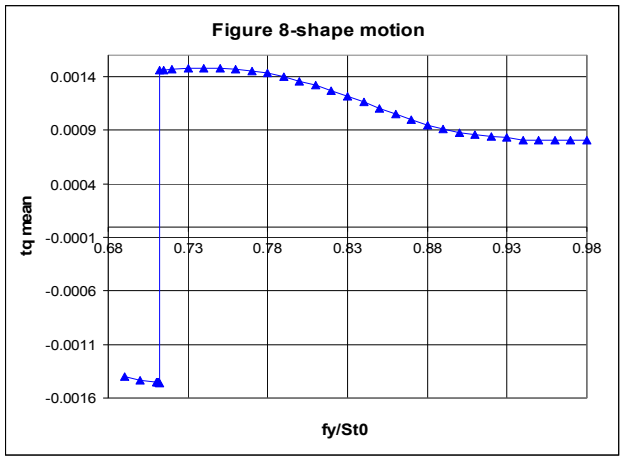

Figure 8. Time-mean value of torque vs. frequency ratio for Re=250

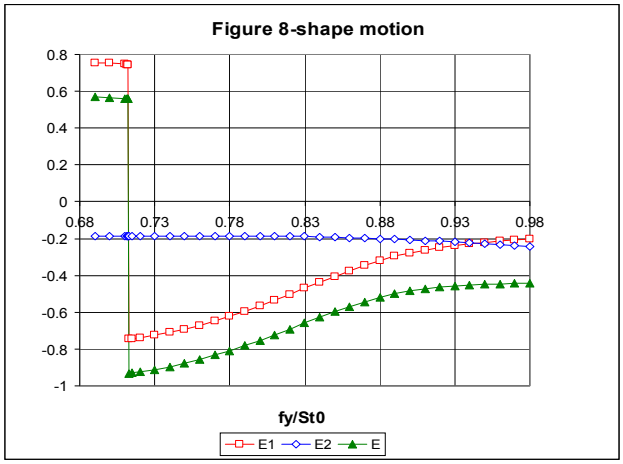

Figure 9. Energy transfer E, E_1, E_2 vs. frequency ratio for Re=250

Pre- and Post-jump Analysis

The vicinity of a jump is investigated by drag-lift limit cycles and vorticity contours. The limit cycle (C_D, C_L) curve shown in Fig. 10 reveals complex curves for the pre-jump curve (thick line) and the post-jump curve (thin line). The difference in frequency ratios is only 0.00001, but a drastic change in the outcome is evident. The curves are mirror images (flipping

along the line of C_L=0), and the direction of orientation of the two curves is also opposite.

The vorticity contours shown in Fig. 11 also show the mirror image nature of the flow before and after a jump. The contours belong to the same cylinder position. The gray lines indicate negative vorticity values, moving clockwise, and the black are positive, rotating counter-clockwise. The vortex shedding mode starts out as P+S, meaning that a pair of vortices and a single vortex are shed in one period. Later, however, the mode seems to shift towards 2S.

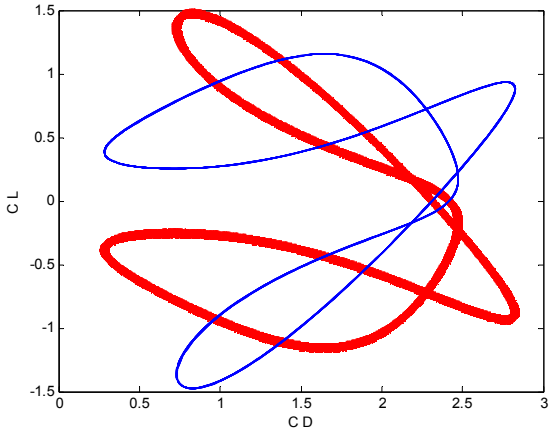

Figure 10. Pre- and post-jump limit cycle (C_D,C_L) curves: thick line - A_x=0.71213, thin line - A_x=0.71214

The vorticity contours shown in Fig. 12 give flow patterns at larger frequency ratios (still under 1), with 'snapshots' taken at the same instant (t=300). Compared to the vorticity contours nearer the vortex switch (Fig. 11), the path is wider and the vortices seem to disperse somewhat earlier as frequency increases. The P+S vortex mode is present near the cylinder.

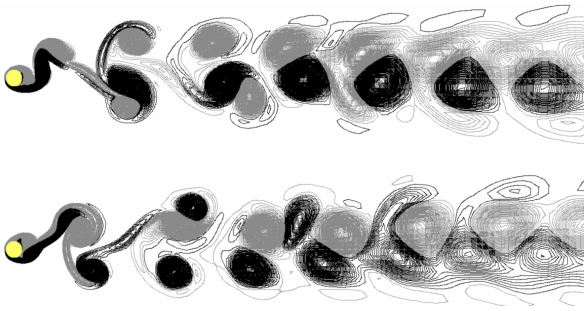

Figure 11. Pre- and post-jump vorticity contours: top - f/St_0=0.71213, bottom - f/St_0=0.71214

The present cylinder-flow system is reflection-symmetric about a line through the cylinder center and parallel to the freestream velocity vector, as shown by both the limit cycle curves and vorticity contours. A physical system that is symmetric is vulnerable to symmetry-breaking bifurcation (Crawford and Knobloch, 1991), which may well be the case here.

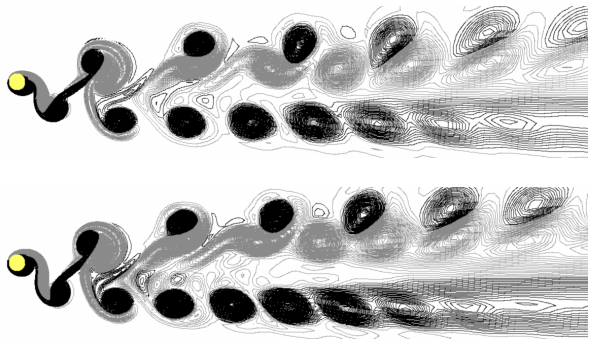

Figure 12. Vorticity contours at two frequency ratios: top - f/St_0=0.85, bottom - f/St_0=0.95

CONCLUSIONS

Cylinder motion in the shape of a slender figure 8 was investigated in this numerical study using a 2D computational method based on the finite difference method. When plotted against in-line amplitude of oscillation, time-mean and rms values of force coefficients at Re=150, 200 and 250 yielded smooth curves and tended to increase with amplitude, although energy transfer decreased and was always negative, meaning that the fluid obtains energy from the cylinder.

When plotted against frequency ratio, the time-mean values of lift and torque showed a jump, a symptom of vortex switching. This was also present in the energy transfer curves, with the pre-jump values being positive, and the post-jump values negative.

Limit cycle curves from before and after a jump were symmetric, mirror images, and quite complex. Vorticity contours also showed a mirror image pre- and post-jump.

In this study, only one orientation was investigated. As Perdikaris et al. (2009) found at Re=400 that orientation influences results, this is one direction for future study. It should be noted that a great deal of computational time is required for a systematic study. Another area of investigation would be to vary the initial condition in order to produce more complete state curves and confirm their symmetric nature.

ACKNOWLEDGMENTS

The support provided by the Hungarian Research Foundation (OTKA Project Nos. K 76085 and K 68207) is gratefully acknowledged. The authors thank Mr. L. Daróczy for designing the flow visualization software.

REFERENCES

Al-Mdallal, Q.M., Lawrence, K.P. and Kocabiyik, S., 2007, "Forced streamwise oscillations of a circular cylinder: Locked-on modes and resulting fluid forces," *Journal of Fluids and Structures* **23**, 681-701.

Baranyi, L., 2003, "Computation of unsteady momentum and heat transfer from a fixed circular cylinder in laminar flow," *Journal of Computational and Applied Mechanics* **4**, 13-25.

Baranyi, L., 2005, "Lift and drag evaluation in translating and rotating non-inertial systems," *Journal of Fluids and Structures* **20**, 25-34,

Baranyi, L., 2008, "Numerical simulation of flow around an orbiting cylinder at different ellipticity values," *Journal of Fluids and Structures* **24**, 883-906.

Baranyi, L., 2009, "Sudden and gradual alteration of amplitude during the computation for flow around a cylinder oscillating in transverse or in-line direction," *ASME 2009 Pressure Vessels and Piping Conference*, *Symposium on Flow-Induced Vibration*. Prague, Paper No. PVP2009-77463.

Blackburn, H.M. and Henderson, R.D., 1999, "A study of two-dimensional flow past an oscillating cylinder," *Journal of Fluid Mechanics* **385**, 255-286.

Cetiner, O. and Rockwell, D., 2001, "Streamwise oscillations of a cylinder in a steady current. Part 1. Locked-on states of vortex formation and loading," *Journal of Fluid Mechanics* **427**, 1-28.

Chakraborty, J., Verma, N. and Chhabra, R.P., 2004, "Wall effects in flow past a circular cylinder in a plane channel: a numerical study," *Chemical Engineering and Processing* **43**, 1529–1537.

Crawford, J.D. and Knobloch, E., 1991, "Symmetry and symmetry-breaking bifurcations in fluid dynamics," *Annual Review of Fluid Mechanics* **23**, 341-387.

Didier, E. and Borges, A.R.J., 2007, "Numerical predictions of low Reynolds number flow over an oscillating circular cylinder," *Journal of Computational and Applied Mechanics* **8**(1), 39-55.

Kravchenko, A.G., Moin, P. and Shariff, K., 1999, "B-Spline method and zonal grids for simulations of complex turbulent flows," *Journal of Computational Physics* **151**, 757–789.

Lu, X.Y. and Dalton, C., 1996, "Calculation of the timing of vortex formation from an oscillating cylinder," *Journal of Fluids and Structures* **10**, 527-541.

Mureithi, N.W., Huynh, K. and Pham, A., 2009, "Low order model dynamics of the forced cylinder wake," *ASME 2009 Pressure Vessels and Piping Conference*, *Symposium on Flow-Induced Vibration*. Prague, Paper No. PVP2009-78093.

Perdikaris, P.D., Kaiktsis, L. and Triantafyllou, G.S., 2009, "Computational study of flow structure and forces on a cylinder vibrating transversely and in-line to a steady stream: Effects of subharmonic forcing," *ASME 2009 Pressure Vessels and Piping Conference*, *Symposium on Flow-Induced Vibration*. Prague, Paper No. PVP2009-78010

Stansby, P. K. and Rainey, R.C.T., 2001, "On the orbital response of a rotating cylinder in a current," Journal of Fluid Mechanics **439**, 87-108.

Williamson, C. H. K. and Roshko, A., 1988, "Vortex formation in the wake of an oscillating cylinder," *Journal of Fluids and Structures* **2**, 355-381.

